TOWARDS A NUMERICAL DISSIPATION FREE SYMMETRY-PRESERVING COLLOCATED METHOD FOR TURBULENT FLOWS

D. Santos[1], **J. Hasslberger**[1], **M. Schweiger**[1], **F.X. Trias**[2], **M. Klein**[1]
[1]Institute of Applied Mathematics and Scientific Computing
University of the Bundeswehr Munich, Germany
{daniel.santos, josef.hasslberger, magnus.schweiger, markus.klein}@unibw.de
[2]Heat and Mass Transfer Technological Center
Polytechnic University of Catalonia, Spain
francesc.xavier.trias@upc.edu

INTRODUCTION

Finite Volume collocated discretizations on unstructured meshes are the predominant approach for solving the Navier–Stokes equations in general-purpose CFD codes such as OpenFOAM and ANSYS Fluent, for the comparatively easy treatment of complex geometries [1]. Compared with staggered arrangements, collocated methods are known to suffer from checkerboarding phenomena [2] and potential stability issues [3, 4]. Checkerboarding is commonly mitigated through the use of a compact Laplacian operator; however, this approach introduces artificial kinetic energy errors that may themselves lead to instability.

Apart from the kinetic energy error associated with the pressure gradient in collocated configurations, an additional temporal error arises from the time integration scheme [5]. Together, these artificial contributions constitute the primary sources of numerical dissipation in collocated arrangements. Excessive numerical dissipation is not appropriate for DNS and LES simulations, as it interferes with the delicate balance between convective transport and physical dissipation. Consequently, reliable numerical methods for DNS/LES should be free of numerical dissipation, or at least exhibit a small and controllable amount.

A collocated symmetry-preserving formulation of the incompressible Navier–Stokes equations was introduced by Trias et al. [1]. Considering a mesh composed of n control volumes and m faces, the semi-discrete governing equations read

$$\Omega\frac{d\mathbf{u}_c}{dt} + \mathbf{C}(\mathbf{u}_s)\mathbf{u}_c = \mathbf{D}\mathbf{u}_c - \Omega\mathbf{G}_c\mathbf{p}_c, \quad (1)$$

$$\mathbf{M}\mathbf{u}_s = \mathbf{0}_c, \quad (2)$$

where $\mathbf{u}_c \in \mathbb{R}^{3n}$ and $\mathbf{p}_c \in \mathbb{R}^n$ denote the cell-centered velocity and pressure, respectively. Face-based quantities, such as the face-centered velocity $\mathbf{u}_s \in \mathbb{R}^m$ are obtained from cell-centered variables through an interpolation operator $\Gamma_{c\to s} \in \mathbb{R}^{m\times 3n}$:

$$\mathbf{u}_s = \Gamma_{c\to s}\mathbf{u}_c. \quad (3)$$

The diagonal matrix $\Omega \in \mathbb{R}^{3n\times 3n}$ contains the cell volumes in its diagonal, $\mathbf{C}(\mathbf{u}_s) \in \mathbb{R}^{3n\times 3n}$ is the discrete convective operator, $\mathbf{D} \in \mathbb{R}^{3n\times 3n}$ is the discrete diffusive operator, $\mathbf{G}_c \in \mathbb{R}^{3n\times n}$ is the cell-to-cell discrete gradient operator and $\mathbf{M} \in \mathbb{R}^{n\times m}$ is the face-to-cell discrete divergence operator.

To ensure unconditional stability when solving the system of equations using a compact Laplacian, a volume-weighted interpolation operator must be employed [3]. This interpolator preserves integrated quantities during the transfer from cell-centered to face-centered variables and can be constructed on arbitrary meshes as follows:

$$\Pi_{c\to s} = \Delta_s^{-1}\Delta_{sc}^T, \quad (4)$$

$$\Gamma_{c\to s} = \mathbf{N}(\mathbf{I}_3 \otimes \Pi_{c\to s}), \quad (5)$$

where $\Pi_{c\to s} \in \mathbb{R}^{m\times n}$ denotes the scalar cell-to-face interpolation operator, and $\mathbf{N} = (N_{s,x}\ N_{s,y}\ N_{s,z}) \in \mathbb{R}^{3m\times m}$. Each matrix $N_{s,i} \in \mathbb{R}^{m\times m}$ is diagonal and contains the x_i components of the face normal vectors. The matrix $\Delta_s \in \mathbb{R}^{m\times m}$ is diagonal and stores the projected distances between adjacent control volumes, while $\Delta_{sc} \in \mathbb{R}^{m\times n}$ contains the projected distances between a cell center and its associated face. A schematic representation of these distances is provided in Fig. 1.

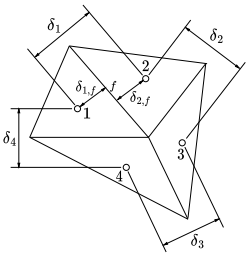

Figure 1: Unstrucutred mesh consisting of four cells. The volume-weighted coefficients for face f are $\delta_{1,f}/\delta_1$ and $\delta_{2,f}/\delta_1$.

KINETIC ENERGY AND SOURCES OF NUMERICAL DISSIPATION

Left multiplying eq. (1) by $\mathbf{u}_c^T$, summing the result with its transpose and using the chain rule we obtain the global discrete kinetic energy equation ($E_k = ||\mathbf{u}_c||^2$):

$$\frac{dE_k}{dt} = -\mathbf{u}_c^T\mathbf{C}(\mathbf{u}_s)\mathbf{u}_c + \mathbf{u}_c^T\mathbf{D}\mathbf{u}_c - \mathbf{u}_c^T\Omega\mathbf{G}_c p_c. \quad (6)$$

Respecting the symmetries of the differential operators is crucial for preserving the physical structure of the governing equations. In the absence of diffusion, i.e., when $\mathbf{D} = \mathbf{0}$, kinetic energy must be conserved. This prop-

erty is satisfied if and only if (1) $\mathbf{C}(\mathbf{u}_s) = -\mathbf{C}(\mathbf{u}_s)^T$, (2) $\mathbf{G} = -\Omega_s^{-1}\mathbf{M}^T$, and (3) $\mathbf{M}_c\mathbf{u}_c = \mathbf{0}_c$. The first condition is ensured by employing a midpoint interpolation (i.e., using 1/2 coefficients) for the transported quantities in the convective operator. The third condition, however, is satisfied only when a Wide-Stencil Laplacian is used, which leads to checkerboarding. In contrast, solving a Compact Laplacian does not exactly satisfy this condition and therefore introduces numerical dissipation. This contribution is ensured to be negative when a volume-weighted interpolation is used [3].

Upon time discretization, an additional source of numerical dissipation is introduced in Eq. (6). Let the discrete approximation of the time derivative $\frac{d\mathbf{u}_c}{dt}$ be denoted by $ddt(\mathbf{u}_c)$. Correspondingly, the discrete time derivative of the kinetic energy is denoted by $ddt(E_k)$. The fully discrete kinetic energy equation can then be written as:

$$\begin{aligned} ddt(E_k) &= -\mathbf{u}_c^T\mathbf{C}(\mathbf{u}_s)\mathbf{u}_c + \mathbf{u}_c^T\mathbf{D}\mathbf{u}_c \\ &- \mathbf{u}_c^T\Omega\mathbf{G}_c p_c + \varepsilon_t, \end{aligned} \tag{7}$$

where $\varepsilon_t = ddt(E_k) - \mathbf{u}_c^T \cdot ddt(\mathbf{u}_c)$. Note that $ddt(E_k) = ddt(0.5||\mathbf{u}_c||^2) \neq \mathbf{u}_c^T \cdot ddt(\mathbf{u}_c)$ in general, so this error arises when the chain rule is not satisfied at the discrete level. The sign of ε_t depends on the time integration scheme and decreases with the time step size according to the order of accuracy of the method, i.e., $\mathcal{O}(\Delta t^n)$.

Let us introduce the following definitions:

$$\varepsilon_\nu = -\mathbf{u}_c^T\mathbf{D}\mathbf{u}_c, \tag{8}$$

$$\varepsilon_C = -\mathbf{u}_c^T\mathbf{C}(\mathbf{u}_s)\mathbf{u}_c \rightarrow R_C = \frac{\varepsilon_C}{|\varepsilon_\nu|}, \tag{9}$$

$$\varepsilon_p = -\mathbf{u}_c^T\Omega\mathbf{G}_c p_c \rightarrow R_p = \frac{\varepsilon_p}{|\varepsilon_\nu|}, \tag{10}$$

$$\varepsilon_t = ddt(E_k) - \mathbf{u}_c^T \cdot ddt(\mathbf{u}_c) \rightarrow R_t = \frac{\varepsilon_t}{|\varepsilon_\nu|}, \tag{11}$$

where ε_ν is the dissipation introduced by the viscous term (which is always negative in a symmetry-preserving scheme), ε_C is the dissipation introduced by the convective term (which is zero up to machine precission in a symmetry-preserving scheme), ε_p is the dissipation introduced by the pressure term and ε_t is the dissipation introduced by the time integration. The different R_i coefficients will allow us to compare the artificial contributions with the physical dissipation.

Several strategies will be investigated to reduce numerical dissipation. Increasing the order of the time integration scheme can significantly reduce ε_t, making ε_p the dominant contribution, as it scales as $\mathcal{O}(\Delta t)$ [3]. To further reduce this latter term, a van Kan projection method [1] will be examined. This projection consists of splitting the pressure at the current time step as $\mathbf{p}_c^{n+1} = \mathbf{p}_c^n + \mathbf{p}_c'$, and solving a Poisson equation for $\mathbf{p}_c'$.

3D TAYLOR GREEN VORTEX AT $Re = 1600$

A numerical test will be performed for the Taylor Green vortex at $Re = 1600$. The initial conditions are given by:

$$U_X = U_0 cos(x) sin(y) sin(z), \tag{12}$$

$$U_Y = -U_0 sin(x) cos(y) sin(z), \tag{13}$$

$$U_Z = 0, \tag{14}$$

and periodic boundary conditions are employed. The characteristic velocity and length scales are $U_0 = 1\,\mathrm{m\,s^{-1}}$ and $l_0 = 1\,\mathrm{m}$, respectively. Figure 2 presents the normalized global kinetic energy, $\hat{E}_k = E_k/U_0^2$, as a function of the normalized time, $\hat{t} = tU_0/l_0$, for an implicit Euler time integration scheme and different Courant numbers, a 32^3 regular mesh and two pressure projection methods. The Chorin Projection (Ch) approach corresponds to the classical pressure projection method, whereas vK denotes the van Kan pressure projection method.

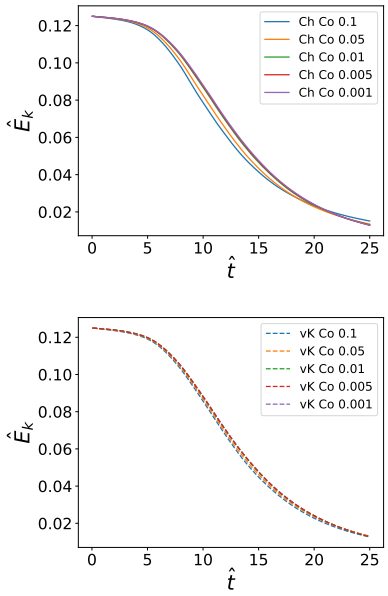

Figure 2: Comparison of the time convergence of kinetic energy spectra for Ch (Chorin Projection method) and vK (van Kan projection method).

As shown in Fig. 2, the vK method reaches temporal convergence significantly faster, at approximately $maxCo = 0.01 - 0.005$, whereas the Ch method requires $maxCo = 0.005 - 0.001$ to achieve convergence (and they both coincide in the time converged limit). This analysis indicates that the dissipation introduced by large time steps through ε_p and ε_t may act as an implicit model. Fig. 3 shows the normalized time evolution of the different ε_i (normalized multiplying them by l_0/U_0^3) for different Courant numbers. ε_C is not shown in the plots because it is virtually 0. As observed in the plots, the Ch method exhibits a higher level of numerical dissipation at larger Courant numbers, which is reflected in lower kinetic energy values (see Fig. 2). For sufficiently small Courant numbers, both ε_p and ε_t tend to zero, and the two solutions converge to the same limit. It is noteworthy that ε_p remains very small for the vK projection method, indicating that this approach substantially reduces the numerical dissipation associated with the pressure term.

To facilitate a direct comparison between numerical and physical dissipation, Fig. 4 presents the coefficients R_i. In the worst case scenario (Ch method with a Courant number of 0.1), the numerical dissipation attributed to the pressure term reaches approximately 40% of the physical dissipation while the numerical dissipation attributed to the time integration term is kept between $10\% - 30\%$.

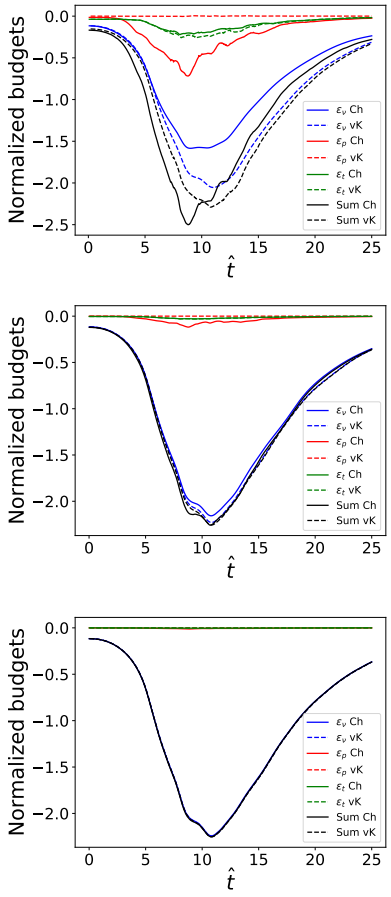

Figure 3: Comparison of the time convergence of the kinetic energy budgets for Ch (Chorin method) and vK (van Kan projection method). (Top) maxCo 0.1. (Middle) maxCo 0.01. (Bottom) maxCo 0.001.

Again, R_p remains insignificant for the vK projection method.

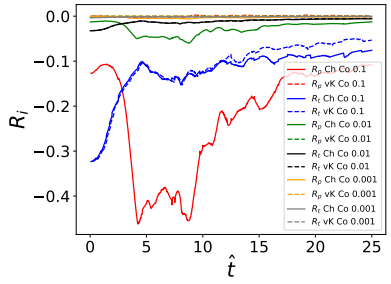

Figure 4: Comparison of the time convergence of the R_i coefficients using a first order implicit Euler.

The vK projection method appears sufficient to nearly eliminate ε_p. While reducing the time step is one possible strategy for decreasing ε_t (and ε_p), this approach is practical only up to a certain limit. An alternative strategy to reduce ε_t is the use of higher-order time integration schemes. Figure 5 presents the coefficients R_i obtained with a second-order backward time integration method. As shown, R_t is significantly reduced and R_p becomes the dominant contribution. For the Ch method, the numerical dissipation reaches nearly 35%, whereas for the vK method it remains close to 0%, rendering the method effectively free of numerical dissipation.

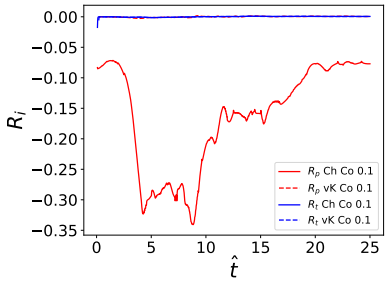

Figure 5: R_i coefficients using a second order time integration scheme.

CONCLUSIONS

This work presents a collocated, virtually dissipation-free, symmetry-preserving Finite Volume method. The proposed approach extends the unconditionally stable symmetry-preserving formulation introduced in [1, 3] by incorporating a van Kan pressure projection method, which nearly eliminates the numerical dissipation associated with the pressure term in collocated arrangements when a compact Laplacian is employed. Numerical experiments indicate that the method is effective in practice, particularly when combined with high-order time integration schemes. A practical application involving a T-junction configuration will be presented at the conference.

ACKNOWLEDGEMENTS

This work was funded by the German Federal Ministry of Research, Technology and Space (BMFTR) under grant number 02NUK071.

REFERENCES

[1] Trias, F.X., Lehmkuhl, O., Oliva, A., Pérez-Segarra, C.D. and Verstappen, R.W.C.P. : Symmetry-preserving discretization of Navier-Stokes equations on collocated unstructured meshes. *Journal of Computational Physics*, **258**, 246-267 (2014).

[2] Hopman, J.A., Santos, D., Alsalti-Baldellou, À., Rigola, J. and Trias F.X. : Quantifying the checkerboard problem to reduce numerical dissipation. *Journal of Computational Physics*, **521**, 113537 (2025).

[3] Santos. D., Hopman, J.A., Pérez-Segarra, C.D., and Trias F.X. : On a symmetry-preserving unconditionally stable projection method on collocated unstructured grids for incompressible flows. *Journal of Computational Physics*, **523**, 113631 (2025).

[4] Felten, F.N., Lund T.S. : Kinetic energy conservation issues associated with the collocated mesh scheme for incompressible flow. *Journal of Computational Physics*, **215**, 465–484 (2006).

[5] Capuano, F., Coppola, G., Rández, L., de Luca, L. : Explicit Runge–Kutta schemes for incompressible flow with improved energy-conservation properties. *Journal of Computational Physics*, **328**, 86-94 (2017).